

FINITE ELEMENT ANALYSIS FOR DYNAMIC RESPONSE OF VISCOELASTIC SANDWICHED STRUCTURES INTEGRATED WITH ALUMINUM SHEETS

Yasser Hamed Elmoghazy^{1,2}, Babak Safaei^{1,2,3}, Saeid Sahmani⁴

¹Nanotechnology and Multifunctional Structures Research Center (NMSRC),
Eastern Mediterranean University, Famagusta, Turkey

²Department of Mechanical Engineering, Eastern Mediterranean University, Famagusta, Turkey

³Department of Mechanical Engineering Science, University of Johannesburg, South Africa

⁴School of Science and Technology, The University of Georgia, Tbilisi, Georgia

Abstract. *Passive vibration attenuation of modern mechanical structures is one of the most essential technologies applied to the arsenal of modern mechanical structures. In this work, dynamics analysis is performed on viscoelastic (VE) sandwich beam and plate by using finite element method. The proposed structure is composed of a VE core and aluminum face sheets as substrate layers on both sides of the structure. Small-strain VE material is modeled based on complex constant moduli model and numerical method is used to develop the finite element (FE) shear model based on first-order shear deformation theory (FSDT) and Hamilton principle. In modal analysis, model-effective mass analysis is performed to investigate its dominant mode shape and sweet spot at resonance using C3D20 and CPS8 elements. The former is indicated as a 3-D element with 20 nodes while the latter is indicated as a 2-D plane strain element with eight nodes. In harmonic analysis, resonance frequency is obtained based on mode superposition method to evaluate the steady-state response of VE sandwich beam via maximum deformation. Thereafter, the results are compared against analytical solutions from the literature. Moreover, a parametric study shows that the natural frequency of the beam did not change with the increase in core thickness. However, normalized loss factor of VE sandwich beam η_n/η_v is directly proportional to VE damping factor η_v and the thickness of VE core layer. Based on frequency response function, the results of resonance frequencies for VE beam are in the range of modal natural frequency.*

Key words: *Viscoelastic, Sandwich Structure, Dynamics Analysis, Complex Constant Moduli, Normalized Loss Factor*

Received: October 04, 2023 / Accepted November 26, 2023

Corresponding author: Babak Safaei

Department of Mechanical Engineering, Eastern Mediterranean University, Famagusta, North Cyprus via Mersin 10, Turkey

Department of Mechanical Engineering Science, University of Johannesburg, Gauteng 2006, South Africa

E-mail: babak.safaei@emu.edu.tr

1. INTRODUCTION

The key parameters to obtain an optimum design of modern mechanical structures with ideal performance are lightweight and noise control which directly lead to the wide applications of thin-walled structures. These structures can be represented as thin beams and thin plates that are extensively used in many engineering applications such as aerospace [1], automobile industry [2], and civil engineering [3]. Since thin-walled structures are "light" and "thin", it is more likely to augment the induced vibrations under external excitations, which compromises the stability of such structures. As a result, the vibration of thin-walled structures must be controlled. One of the approaches to the problem is to use active piezoelectric elements which may offer an optimal damping performance of thin-walled structures since it includes the ability of sensing and actuation control [4]. Applying a damping layer to thin-walled structures to control their vibrations is a widely utilized strategy in engineering practice [5]. Among them, viscoelastic (VE) materials, which have good damping qualities, are most widely applied in structural vibration as a passive damping treatment [6, 7]. A typical passive damping treatment structure consists of two elastic layers and a VE core sandwiched between constraining layer and base beam. The VE core allows vibration energy to dissipate through a cyclic deformation, while the main advantage of constraining layer is to increase periodic shear deformation and stress resistance of the core, hence directly leading to an increase in damping energy within VE core [8].

In engineering practice, sandwich structures have complex geometric shapes and boundary conditions thus, such problems cannot be effectively solved by the conventional analytical process, accordingly finite element (FE) approach is commonly used which may facilitate the computational complexity of such problem [9–12]. Arvin et al. [13] developed four nodes VE sandwich beam element based on higher-order shear deformation theory to explore the steady-state and transient responses of a VE composite sandwich beam. Wang and Inman [14] developed a 2D FE model to study the dynamic performance of a hybrid composite sandwich beam by using VE Golla–Hughes model (GHM). Lin and Rao [15] proposed FE model for vibration performance of VE multiple-layered sandwich beam by incorporating VE Biot model into FE model. Reddy and Panda [16] developed FE model to explore the nonlinear frequency response for harmonically excited VE sandwich beam based on harmonic balance method considering different VE constitutive models. Jahan et al. [17] performed FE modal study to examine the effectiveness and influential parameters of a passive rail damper system using lab-scaled model. Araújo et al. [18] proposed FE model to explore the dynamic response of active-passive hybrid sandwich plate using mixed layerwise approach.

Although FE models have been widely used in the dynamic modeling of complex structures, some FE models are difficult to implement, thus some researchers have tried to ensure accurate modeling based on searching for ways to improve computational efficiency, such that, some models between the analytical method and the FE method, called semi-analytical semi-numerical method. Lewandowski and Baum [19] developed mixed model to anticipate the free vibration response of VE sandwich beam using virtual work principle and VE Zener model. Daya and Potier-Ferry [20] established a shell FE model using homotopy algorithm and asymptotic method to solve the nonlinear eigenvalue problem of VE sandwich structures. Koutsawa et al. [21] investigated the non-linear behavior of a laminated glass beam by applying asymptotic numerical technique to establish a diamond toolbox. The performance of the diamond toolbox was demonstrated numerically and experimentally. Also, Lampoh et al. [22] performed sensitivity studies on the non-linear mechanical behavior of VE laminated glass beam.

Recently, small-size composite structures with VE material have been explored by many researchers. For instance, Loghman et al. [23] used finite difference method coupled with Galerkin bases to examine the size-dependent vibration behavior of a VE micro-beam employing modified couple stress theory (MCST). Li et al. [24] analytically and experimentally investigated the nonlinear vibration response of multiple layered VE composite sandwich plate and the equation of motion derived based on von Karman approach. Their analytical model was developed based on strain energy principle and validated against experimental nonlinear vibration characteristics. Rahmani et al. [25] utilized a comprehensive mathematical-mechanical model based on higher-order, nonlocal Eringen's theory, and MCST theory to explore the wave propagation of rotating VE nanobeams including the influence of many parameters on wave propagation frequencies, such as nonlocal parameter and thermal gradient. Yuan et al. [26] studied the dynamic stability of FGM composite microcells integrated with a nonlinear VE foundation under size-dependent gradient. Jalaei et al. [27] proposed the transient response of small-size visco-porous FG structure exposed to transverse loads and magnetic field based on Eringen's nonlocal strain gradient theory. Youzera et al. [28] proposed an applicable analytical model for the forced vibration analysis and nonlinear associated loss factor of VE-FGM composite beam by using zig-zag theory coupled with HSDT. The governing sixth-order differential equilibrium equation of motion is derived using virtual work principle. Karimi et al. [29] established a numerical approach based on modal stability procedure (MSP) to explore the vibroacoustic behavior of sandwich beam integrated with frequency and temperature-dependent VE core.

Hereby, research methodology for dynamic analysis of VE sandwich structures is proposed by using finite element method. In the pre-processing step, the integral FE shear beam element is developed based on first-order shear deformation theory (FSDT) since the VE core layer demonstrates considerable shear deformation behavior under different loading conditions. The beam's equation of motion is derived based on Hamilton principle. The numerical results are compared against analytical models from previous literature. Further, the steady-state frequency response is obtained for optimizing the design and ensuring the structural integrity of such system. This work aims to achieve an appropriate design for both VE beam and plate with integrated Aluminum sheets by investigating their damping characteristics, including the effects of VE loss factor η_v and thickness of the VE core layer.

2. SHEAR MODEL KINEMATICS RELATIONSHIPS

The geometric configurations and deformation of typical VE sandwich beams are demonstrated in Fig. 1. Here, h_1 , h_2 and H are the thickness of upper layer, lower layer and the total thickness of the VE sandwich beam, respectively, and L is the span of VE sandwich beam. The shear strain of VE layer γ_{xz} and rotation of VE sandwich beam θ could be expressed as [30]:

$$\gamma_{xz} = \theta + \varphi_x \quad (1)$$

where φ_x is the shear angle of VE core since the two elastic layers are treated as Euler-Bernoulli beams neglecting shear deformation.

To simplify FE modeling and formulation the following basic assumptions are proposed:

1. Shear deformation is negligible for elastic layers.
2. The vibrations of the VE sandwich beam is dissipated through periodic shear deformation of the VE layer.
3. All layers of VE sandwich beam have the same transverse displacement w .
4. All layer interaction is constrained.
5. VE material is considered as small strain linear VE.

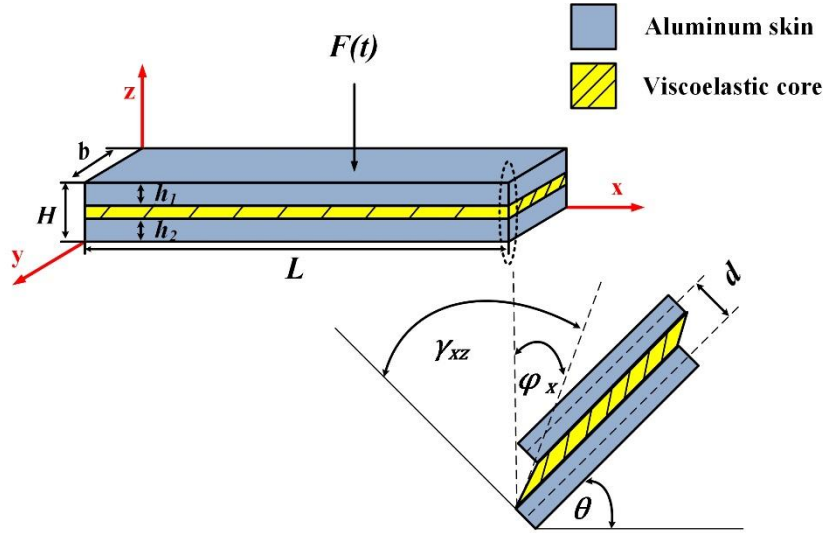


Fig. 1 Passive damping treatment illustration for typical VE sandwich beam with a deformed shear configuration

Axial and transverse displacements $u^{(i)}(x, z, t)$, $w^{(i)}(x, z, t)$ respectively, at any point within the elastic layers could be expressed as [31]:

$$\left. \begin{aligned} u^{(i)}(x, z, t) &= u_i(x, t) - z_i \frac{\partial w_i(x, t)}{\partial x} \\ w^{(i)}(x, z, t) &= w_i(x, t) \end{aligned} \right\} i = c, b \quad (2)$$

where $u_i(x, t)$ and $w_i(x, t)$ are the axial and transverse displacements, at the centroid point of elastic layers, respectively. The relative kinematics relations of VE core shear strain γ_{xz} and axial displacement u_v can be derived using local coordinate system and FSDT [32] as:

$$u_v = \frac{1}{2}(u_c + u_b) + \frac{1}{4}(h_1 - h_2) \frac{\partial w}{\partial x} \quad (3)$$

$$\gamma_{xz} = \frac{1}{H - (h_1 + h_2)} \left[(u_c - u_b) + \left(\frac{h_1 + h_2}{2} + (H - (h_1 + h_2)) \right) \frac{\partial w}{\partial x} \right] \quad (4)$$

3. FINITE ELEMENT MODELLING

3.1. Degrees of Freedom and Shape Functions of Proposed Beam Model

The Integral shear beam element with two nodes i and j is shown in Fig. 2. Each node had four DOF with lateral displacement w along z -direction, rotation θ about x -axis, and axial displacements of elastic layers u_c and u_b . The total set of element nodal displacements $\{d^e\}$ are given as:

$$\{d^e\} = \begin{Bmatrix} d_i \\ d_j \end{Bmatrix} = \{w_i \ \theta_i \ u_{bi} \ u_{ci} \ w_j \ \theta_j \ u_{bj} \ u_{cj}\}^T \tag{5}$$

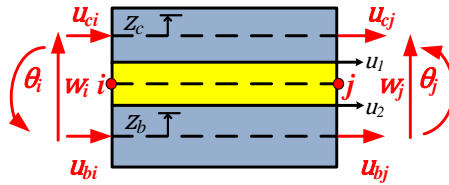


Fig. 2 Integral shear beam element

The transverse displacement field $w(x)$, rotation field $\theta(x) = \frac{\partial w}{\partial x}$, and axial displacement field of elastic layers $u_b(x)$ and $u_c(x)$ are expressed as a cubic polynomial function:

$$w(x) = c_0 + c_1s + c_2s^2 + c_3s^3 \tag{6}$$

$$\theta(x) = c_1 + 2c_2s + 3c_3s^2 \tag{7}$$

$$u_b(x) = c_4 + c_5s, \ u_c(x) = c_6 + c_7s \tag{8}$$

where $s = x/l_e$ represents the normalized coordinate with l_e being equivalent element length. From Eqs. (6), (7), and (8) The element displacement field within the element could be expressed in matrix form as:

$$\begin{Bmatrix} w \\ \theta \\ u_b \\ u_c \end{Bmatrix} = [T]\{c\} = \begin{bmatrix} 1 & s & s^2 & s^3 & 0 & 0 & 0 & 0 \\ 0 & \frac{1}{l_e} & \frac{2s}{l_e} & \frac{3s^2}{l_e} & 0 & 0 & 0 & 0 \\ 0 & 0 & 0 & 0 & 1 & s & 0 & 0 \\ 0 & 0 & 0 & 0 & 0 & 0 & 1 & s \end{bmatrix} \begin{Bmatrix} c_0 \\ c_1 \\ c_2 \\ c_3 \\ c_4 \\ c_5 \\ c_6 \\ c_7 \end{Bmatrix} \tag{9}$$

where $s = x/l_e$ represents the normalized coordinate with l_e being equivalent element length. $\{c\}$ and $[T]$ are the coefficient matrix and polynomial matrix, respectively which can be represented by element nodal displacements $\{d^e\}$ explicitly in matrix form as [32]:

$$\{d\} = [T]\{c\} = [T][Q^{-1}]\{d^e\} = [N]\{d^e\} \tag{10}$$

where N is the shape function matrix corresponding to the four nodal DOF of each node in the form of 4×8 matrix and Q is 8×8 matrix that depends on the applied boundary condition. Using Eq. (10) and applying the C-F boundary condition, the Q matrix is obtained in a matrix form as:

$$Q = \begin{bmatrix} 1 & 1 & 1 & 1 & 0 & 0 & 0 & 0 \\ 0 & \frac{1}{l_e} & \frac{2}{l_e} & \frac{3}{l_e} & 0 & 0 & 0 & 0 \\ 0 & 0 & 0 & 0 & 1 & 1 & 0 & 0 \\ 0 & 0 & 0 & 0 & 0 & 0 & 1 & 1 \\ 1 & 0 & 0 & 0 & 0 & 0 & 0 & 0 \\ 0 & \frac{1}{l_e} & 0 & 0 & 0 & 0 & 0 & 0 \\ 0 & 0 & 0 & 0 & 1 & 0 & 0 & 0 \\ 0 & 0 & 0 & 0 & 0 & 0 & 1 & 0 \end{bmatrix} \quad (11)$$

The shape function is obtained after the decoupling-inversion operation using Q^{-1} as:

$$[N_x \quad N_x' \quad N_1 \quad N_2]^T = TQ^{-1} \quad (12)$$

The generalized shape function matrix is obtained as a column matrix [13]:

$$N_x = \begin{bmatrix} 1 - 3s^2 + 2s^3 \\ x - \frac{2x^2}{l_e} + \frac{x^3}{l_e^2} \\ 0 \\ 0 \\ 3s^2 - 2s^3 \\ \frac{x^3}{l_e^2} - \frac{x^2}{l_e} \\ 0 \\ 0 \end{bmatrix}^T, \quad N_x' = \begin{bmatrix} 6\left(\frac{x^2}{l_e^3} - \frac{x}{l_e^2}\right) \\ 1 - 4s + 3s^2 \\ 0 \\ 0 \\ -6\left(\frac{x^2}{l_e^3} - \frac{x}{l_e^2}\right) \\ -2s + 3s^2 \\ 0 \\ 0 \end{bmatrix}^T, \quad N_1 = \begin{bmatrix} 0 \\ 0 \\ 1 - s \\ 0 \\ 0 \\ 0 \\ s \\ 0 \end{bmatrix}^T, \quad N_2 = \begin{bmatrix} 0 \\ 0 \\ 0 \\ 1 - s \\ 0 \\ 0 \\ 0 \\ s \end{bmatrix}^T$$

The displacements filed within the element could be then determined by the nodal displacement of element through shape functions interpolation:

$$w = N_x d^e, \quad \theta = N_x' d^e, \quad u_b = N_1 d^e, \quad u_c = N_2 d^e, \quad u_v = N_3 d^e, \quad \gamma = N_4 d^e$$

where N_3 and N_4 were derived based on the relative kinematics relations γ_{xz} and u_v in Eqs. (3) and (4) as follows:

$$N_3 = \frac{1}{2} \left[(N_1 + N_2) + \left(\frac{h_1 + h_3}{2} \right) N_x' \right] \quad (13)$$

$$N_4 = \frac{1}{H - (h_1 + h_2)} \left[(N_2 - N_1) + \left(\frac{h_1 + h_3}{2} + (H - (h_1 + h_2)) \right) N_x' \right] \quad (14)$$

3.2. Element Stiffness Matrix

The principle of strain energy can be applied to obtain element stiffness matrix of VE sandwich beam. In general, the elastic strain energy is expressed as:

$$U = \int_V \frac{\sigma^2}{2E} dV \quad (15)$$

3.2.1. Strain Energy due to Axial Loading

Based on Eq. (15), the strain energy due to axial loading of elastic layer U_a is:

$$U_a = \frac{EA}{2} \int \varepsilon^2 dx \quad (16)$$

The definition of axial strain was defined as the rate change of the displacement:

$$\varepsilon = \frac{\partial u}{\partial x} \quad (17)$$

Substituting Eq. (17) into Eq. (16) yields [32]:

$$U_a = \frac{1}{2} EA \int_0^{l_e} \left(\frac{\partial u}{\partial x} \right)^2 dx = \frac{1}{2} d^{eT} K_{ei}^e d^e \quad (18)$$

$$U_{ac} = \frac{1}{2} E_c A_c \int_0^{l_e} \left(\frac{\partial u_c}{\partial x} \right)^2 dx = \frac{1}{2} d^{eT} K_{ec}^e d^e \quad (19)$$

$$U_{ab} = \frac{1}{2} E_b A_b \int_0^{l_e} \left(\frac{\partial u_b}{\partial x} \right)^2 dx = \frac{1}{2} d^{eT} K_{eb}^e d^e \quad (20)$$

The element stiffness matrix of base and constraining layers, corresponding to axial strain energy K_{ab}^e and K_{ac}^e , respectively can be expressed as:

$$K_{ab}^e = E_b A_b \int_0^{l_e} \left[\frac{\partial N_1}{\partial x} \right]^T \left[\frac{\partial N_1}{\partial x} \right] dx \quad (21)$$

$$K_{ac}^e = E_c A_c \int_0^{l_e} \left[\frac{\partial N_2}{\partial x} \right]^T \left[\frac{\partial N_2}{\partial x} \right] dx \quad (22)$$

3.2.2. Strain Energy due to Bending Loading

The elastic strain energy due to flexural bending in the beam is given by:

$$U_b = \int_V \frac{M^2(x) y^2}{2EI^2} dV \quad (23)$$

The flexural bending of the element is given by:

$$\frac{M(x)}{EI} = \frac{\partial^2 w}{\partial x^2} \quad (24)$$

Substituting Eq. 24 into Eq. 23, the bending strain energy of elastic layers is given as:

$$U_b = \frac{E}{2} \iint \left(\frac{\partial^2 w}{\partial x^2} \right)^2 y^2 dA dx \quad (25)$$

$$U_b = \frac{1}{2} EI \int \left(\frac{\partial^2 w}{\partial x^2} \right)^2 dx = \frac{1}{2} d^{eT} K_b^e d^e \quad (26)$$

$$U_{bc} = \frac{1}{2} E_c I_c \int_0^{l_e} \left(\left(\frac{\partial^2 w}{\partial x^2} \right)^2 \right) dx = \frac{1}{2} d^{eT} K_{bc}^e d^e \quad (27)$$

$$U_{bb} = \frac{1}{2} E_b I_b \int_0^{l_e} \left(\left(\frac{\partial^2 w}{\partial x^2} \right)^2 \right) dx = \frac{1}{2} d^{eT} K_{bb}^e d^e \quad (28)$$

The element stiffness matrix of constraining and base layers, corresponding to bending strain energy K_{bc}^e and K_{bb}^e , respectively can then be expressed as:

$$K_{bb}^e = E_b I_b \int_0^{l_e} \left[\frac{\partial N_x}{\partial x} \right]^T \left[\frac{\partial N_x}{\partial x} \right] dx \quad (29)$$

$$K_{bc}^e = E_c I_c \int_0^{l_e} \left[\frac{\partial N_2}{\partial x} \right]^T \left[\frac{\partial N_2}{\partial x} \right] dx \quad (30)$$

3.2.3. Strain energy due to shear loading

Strain energy due to shear loading can be derived as

$$U_{shear} = \int \frac{\tau^2}{2G} dv = \frac{G\gamma^2}{2} \int dv \quad (31)$$

$$U_{shear} = \frac{G^*\gamma^2}{2} \iint dA dx \quad (32)$$

$$U_{shear} = \frac{1}{2} G^* A_v \int_0^{l_e} \gamma^2 dx = \frac{1}{2} d^{eT} K_s^e d^e \quad (33)$$

K_s^e is the shear element stiffness matrix associated with shear strain energy such that:

$$K_s^e = G^* A_v \int_0^{l_e} N_4^T N_4 dx \quad (34)$$

The total elastic element stiffness matrix K_e^e can be expressed as:

$$K_e^e = K_{eb}^e + K_{ec}^e + K_{bb}^e + K_{bc}^e \quad (35)$$

The element stiffness matrix then could be expressed as:

$$\underbrace{K_e^e}_{[8 \times 8]} = \begin{bmatrix} [K_{eb}^e] & [K_{bb}^e] \\ [K_{bc}^e] & [K_{ec}^e] \end{bmatrix} + \underbrace{K_s^e}_{[8 \times 8]} \quad (36)$$

where K^e is the total element stiffness matrix obtained as the summation of elastic element stiffness matrix K_e^e and shear stiffness element matrix K_s^e of VE sandwich beam.

3.3. Element Mass Matrix

To obtain the element mass matrix, the principle of kinetic energy is applied. By considering the axial and rotational loading associated with kinetic energy, the total kinetic energy T of VE sandwich beam is evaluated as:

$$T = \frac{1}{2} (\rho_c A_c + \rho_v A_v + \rho_b A_b) \int \dot{w}^2 dx + \frac{1}{2} (\rho_c A_c + \rho_v A_v + \rho_b A_b) \int \dot{u}^2 dx \quad (37)$$

The kinetic energy corresponding to the axial and bending loading of each layer is:

$$T_{ac} = \frac{1}{2} \rho_c A_c \int_0^{l_e} \left(\frac{\partial u_c}{\partial t} \right)^2 dx = \frac{1}{2} \dot{d}^{eT} M_{ec}^e \dot{d}^e \quad (38)$$

$$T_{bc} = \frac{1}{2} \rho_c A_c \int_0^{l_e} \left(\frac{\partial w}{\partial t} \right)^2 dx = \frac{1}{2} \dot{d}^{eT} M_{bc}^e \dot{d}^e \quad (39)$$

$$T_{ab} = \frac{1}{2} \rho_b A_b \int_0^{l_e} \left(\frac{\partial u_b}{\partial t} \right)^2 dx = \frac{1}{2} \dot{d}^{eT} M_{eb}^e \dot{d}^e \quad (40)$$

$$T_{bb} = \frac{1}{2} \rho_b A_b \int_0^{l_e} \left(\frac{\partial w}{\partial t} \right)^2 dx = \frac{1}{2} \dot{d}^{eT} M_{bb}^e \dot{d}^e \quad (41)$$

$$T_{av} = \frac{1}{2} \rho_v A_v \int_0^{l_e} \left(\frac{\partial u_v}{\partial t} \right)^2 dx = \frac{1}{2} \dot{d}^{eT} M_{ec}^e \dot{d}^e \quad (42)$$

$$T_{bv} = \frac{1}{2} \rho_v A_v \int_0^{l_e} \left(\frac{\partial w}{\partial t} \right)^2 dx = \frac{1}{2} \dot{d}^{eT} M_{bv}^e \dot{d}^e \quad (43)$$

where T_{ac} , T_{ab} and T_{av} are kinetic energies of the constraining, base, and core layers that correspond to axial loading, respectively. T_{bc} , T_{bb} and T_{bv} are kinetic energies of constraining, base, and core layers corresponding to bending loading, respectively.

The element mass matrices associated with elastic layers and VE core layer corresponding to axial and bending loading M_{ac}^e , M_{bc}^e , M_{ab}^e , M_{bb}^e , M_{av}^e and M_{bv}^e are expressed using the element shape functions as:

$$M_{ac}^e = \rho_c A_c \int_0^{l_e} N_2^T N_2 dx, M_{bc}^e = \rho_c A_c \int_0^{l_e} N_x^T N_x dx \quad (44)$$

$$M_{ab}^e = \rho_b A_b \int_0^{l_e} N_1^T N_1 dx, M_{bb}^e = \rho_b A_b \int_0^{l_e} N_x^T N_x dx \quad (45)$$

$$M_{av}^e = \rho_v A_v \int_0^{l_e} N_3^T N_3 dx, M_{bv}^e = \rho_v A_v \int_0^{l_e} N_x^T N_x dx \quad (46)$$

The element mass matrix M^e is given as:

$$\underbrace{M^e}_{[8 \times 8]} = M_{ac}^e + M_{bc}^e + M_{ab}^e + M_{bb}^e + M_{av}^e + M_{bv}^e \quad (47)$$

3.4. Finite Element Equation of Motion

After assembling the global stiffness and mass matrix of the structure, the Hamilton variation principle is used to derive the dynamic equation of the VE sandwich beam:

$$\int_{t_1}^{t_2} \delta(T - U) dt + \int_{t_1}^{t_2} \delta w dt = 0 \quad (48)$$

After applying Eq. (48), The VE sandwich beam equation of motion is expressed as:

$$M^e \ddot{d}^e + K_e^e d^e + K_v^e d^e = F^e \quad (49)$$

3.5. Linear Vibration Eigenvalue Problem (Constant Complex Modulus)

The complex constant elastic modulus of VE material E is expressed as:

$$E^* = E' + jE'' \quad (50)$$

where E' is the real part, also called storage modulus, and E'' is the imaginary part which is called energy dissipation modulus. $\eta_v = \frac{E''}{E'}$ is VE loss factor, which is the ratio of energy dissipation modulus to storage energy modulus.

The loss factor of VE material physically represents the ratio of the energy consumed from VE material to total energy.

Many researchers have used constant shear complex modulus to obtain a simple dynamic equation by applying a simple harmonic excitation force [33] and Eq. (49) could be expressed as:

$$M^e \dot{d}^e + d^e K^e = 0 \quad (51)$$

where K^e , M^e are the total stiffness matrix and total mass matrix of the VE sandwich beam, respectively. Then, the eigenvalue problem is expressed as

$$(K^e - \omega^{*2} M^e) X = 0 \quad (52)$$

where ω^* is the complex frequency, and X is the complex eigenmodes of VE sandwich beam. Natural frequency ω_n and model loss factor η_n are calculated as follows:

$$\omega_n = \sqrt{Re \omega^*} \quad (53)$$

4. NUMERICAL RESULTS AND VALIDATION

4.1. Normal Mode Analysis (Free Vibration)

Normal modal analysis is a prerequisite step in modeling the dynamic behavior of VE sandwich structures. It is a semi-final step that gives theoretical values for eigenvalues and eigenvectors that have no physical meaning unless normal model analysis is paired with harmonic or time response analysis. The mechanical and geometrical properties of elastic and core layers of VE sandwich beam are summarized in Table 1.

Table 1 Materials mechanical properties and geometrical specifications of VE sandwich beam [33]

	Aluminum layers	VE core layer
Young modulus (MPa)	6.9×10^4	$1.794 \times (1+0.3i)$
Poisson's ration	0.3	0.3
Loss factor	-	0.1,0.6,1,1.5
Density (kg/m ³)	2766	968.1
Length (mm)	177.8	177.8
Width (mm)	12.7	12.7
Thickness (mm)	1.52	0.127

4.1.1. Case Study #1: C-F VE Sandwich Beam

To study the linear vibration of VE sandwich structures, a cantilever beam was discretized into 30 elements. In this case, VE material is independent from Young's modulus E . The mechanical and geometrical properties of elastic and core layers of VE sandwich beam are summarized in Table 1.

A MATLAB code was developed to solve the eigenvalues problem. In addition, 2D and 3D finite element models were built using FE solver software Abaqus to show the efficiency of the numerical approach.

For mesh modeling, 2D and 3D FE models were built using Abaqus software. The eight-node continuum quadratic brick element CPS8 is used to discretize the 2D model, while the 20-node C3D20 was used to discretize the 3D model.

The sizing control technique is used with a maximum mesh global size of 0.5 mm and maximum deviation factor of 0.1. Table 1 gives the specifications of CPS8 and C3D20.

Based on Euler-Bernoulli beam theory, the natural frequencies of a base beam without VE core and constraining layer are calculated as:

$$\omega_n = \frac{A_n}{2\pi L^2} \sqrt{\frac{EI}{\rho A}} \quad (54)$$

where E is the modulus of elasticity, I is the cross-sectional moment of inertia of the base beam, ρ is material density, and A is the cross-sectional area of the beam. According to Eq. (54), the first fundamental natural frequencies of the base beam without VE core and constraining layer are calculated as 38.83Hz and 247.1Hz.

It is worth pointing out that, with the addition of a VE layer and a constrained layer, the stiffness and mass are increased accordingly. From Eq. (54), an increase in structure stiffness leads to an increase in the natural frequency of the structure, while an increase in the additional mass leads to a decrease in the natural frequency.

According to Table 1, the density of VE core is about half of elastic layer's density, however, the stiffness of the VE core is almost negligible compared to stiffness of the elastic layers. Accordingly, the effect of the additional mass on the natural frequency is much greater than the effect the additional stiffness.

For the sake of comparison, the first six natural frequencies and normalized loss factor of VE sandwich beam were calculated using three different elements based on shear energy consumption assumption when the loss factor $\eta_v = [0.1, 0.6, 1.5]$.

Table 2 Mesh specifications of CPS8 and C3D20 elements implemented in Abaqus

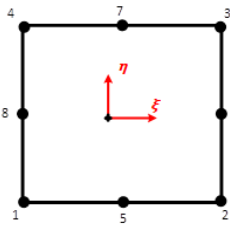
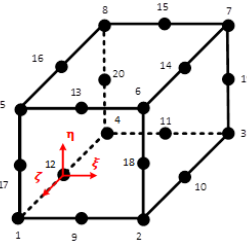
Element	Description	Schematic	NDOF/node
CPS8	<ul style="list-style-type: none"> ▪ Continuum biquadratic. ▪ 8-nodes. ▪ Plane stress 		2 Translations
C3D20	<ul style="list-style-type: none"> ▪ Continuum quadratic brick. ▪ 20-nodes. 		3 Translations

Table 3 shows that FE shear models, real eigenmodes (RM) and asymptotic numerical method (ANM) all had good accuracy in calculating the first six natural frequency of VE sandwich beam under C-F boundary condition against the analytical solution [34]. Table 4 shows normalized loss factor of C-F VE sandwich beam with different η_v .

In comparison, the accuracy of FE shear model was the highest compared with the analytical method [34], the error range was 0-0.15% followed by C3D20 element with an error range of 0-5.918% and an average error of 0.2%; CPS8 element was the third with an error range of 0-6.565% and an average error of 0.858% and RM method had the lowest accuracy, with the lowest error value of 0%, the highest error value of 8.892% and an average error of 0.97%.

Although RM approach had a slightly higher average error than ANM method, RM method could not be deemed accurate. Because RM approach only considers the real part of natural frequency, which contradicts reality. Although the prediction results of natural frequency by RM method were close to analytical solutions when the loss factor η_v was small but when the loss factor η_v was increased to 1.5, the prediction error of natural frequency reached 8.892%. On the other hand, the prediction error of ANM for natural frequency was very consistent and did not fluctuate much, thus the calculated loss factor of ANM for natural frequency was generally accurate. As a result, the prediction accuracies of the five numerical approaches for the natural frequency of C-F VE sandwich beam in this work were ranked as follows: Integral shear element > C3D20 > CPS8 > ANM > RM.

Table 3 Linear frequencies of the C-F VE sandwich beam with different η_v

η_v	Analytical [34]	CPS8	FE Model	RM [35]	C3D20	ANM [36]
	$\omega_n(Hz)$	$\omega_n(Hz)$	$\omega_n(Hz)$	$\omega_n(Hz)$	$\omega_n(Hz)$	$\omega_n(Hz)$
0.1	64.1	64.1	64.1	64.1	64.5	64.5
	296.4	296.5	296.3	296.6	298.6	298.9
	743.7	743.6	743.4	744.3	750.1	746.5
	1393.9	1392.6	1393.4	1395.2	1408.3	1407.7
	2261.1	2256.7	2260.2	2263.4	2288.4	2286.2
	3343.6	3332.8	3342.3	3347.3	3388.7	3385.7
0.6	65.5	64.3	65.4	64.1	64.7	65.9
	298.9	297.4	298.8	296.6	299.5	303.1
	745.5	744.5	745.2	744.3	751	752.3
	1394.9	1393.1	1394.3	1395.2	1409	1412.7
	2261.7	2257	2260.8	2263.4	2289	2290.6
	3344	3333	3342.6	3374.3	3389	3389.5
1	67.4	64.7	67.4	64.1	65.1	67.8
	302.8	299.1	302.7	296.6	301	309.1
	748.6	746.1	748.4	744.3	753	761.1
	1396.6	1394	1396	1395.2	1410	1420.6
	2262.8	2257.6	2261.9	2263.4	2289	2297.9
	3345	3333.3	3343.4	3374.3	3389	3395.9
1.5	69.8	65.5	69.9	64.1	65.9	67.8
	308.8	302.3	308.7	296.6	304	309.1
	754	749	754.2	744.3	756	761.1
	1399.7	1395.8	1399.1	1395.2	1412	1420.6
	2265	2258.7	2264.1	2263.4	2290	2297.9
	3346	3333.9	3344.7	3374.3	3390	3395.9
Average Error (%) \approx		0.858	0.03	0.94	0.2	0.97

Table 4 shows that the accuracy of the FE shear element models implemented in this study is very high in predicting model loss factor for the first six modes of VE sandwich beam structure. With an error range of 0% to 11.45% and an average error of 2.38%, ANM [36] was the most accurate one. In addition, C3D20 element had an error range of 0-14.7%, with an average of 4.19%, which placed it second. RM [35], which had a minimum error of 0% and a maximum error of 8.892%, had the lowest accuracy.

The results showed a significant improvement in the overall damping performance of the C-F VE sandwich beam as the loss factor η_v was increased. When low frequencies were close to loading frequencies, they could generate huge amplitudes, causing what is known as resonance.

Table 4 Normalized loss factor of C-F VE sandwich beam with different η_v

η_v	Analytical [34]	CPS8	RM [35]	C3D20	ANM [36]
	η_n/η_v	η_n/η_v	η_n/η_v	η_n/η_v	η_n/η_v
0.1	0.281	0.283	0.283	0.282	0.281
	0.242	0.242	0.243	0.241	0.242
	0.154	0.154	0.154	0.153	0.154
	0.088	0.089	0.089	0.088	0.089
	0.057	0.057	0.057	0.056	0.057
	0.039	0.039	0.039	0.038	0.039
0.6	0.246	0.281	0.283	0.280	0.247
	0.232	0.241	0.243	0.239	0.224
	0.152	0.154	0.154	0.152	0.150
	0.088	0.089	0.089	0.088	0.088
	0.057	0.057	0.057	0.056	0.057
	0.039	0.039	0.039	0.038	0.039
1	0.202	0.277	0.283	0.276	0.204
	0.217	0.238	0.243	0.236	0.201
	0.150	0.153	0.154	0.152	0.142
	0.088	0.089	0.089	0.088	0.086
	0.057	0.057	0.057	0.056	0.057
	0.038	0.039	0.039	0.038	0.037
1.5	0.153	0.271	0.283	0.270	0.155
	0.197	0.232	0.243	0.231	0.176
	0.146	0.152	0.154	0.150	0.131
	0.087	0.088	0.089	0.087	0.083
	0.056	0.057	0.057	0.056	0.056
	0.038	0.039	0.039	0.038	0.039
Average Error (%) \approx		5.42	6.02	4.19	2.38

Fig. 3 shows relative changes in normalized deflection amplitudes for the first three eigenmodes of C-F VE sandwich beam with a different loss factor $\eta_v = [0.1, 0.6, 1.5]$. It could be noticed that both real and imaginary parts had different amplitudes but the same mode shapes.

For high loss factor η_v , the imaginary part of the complex eigenmodes was significant which affected the damping performance of the whole structure.

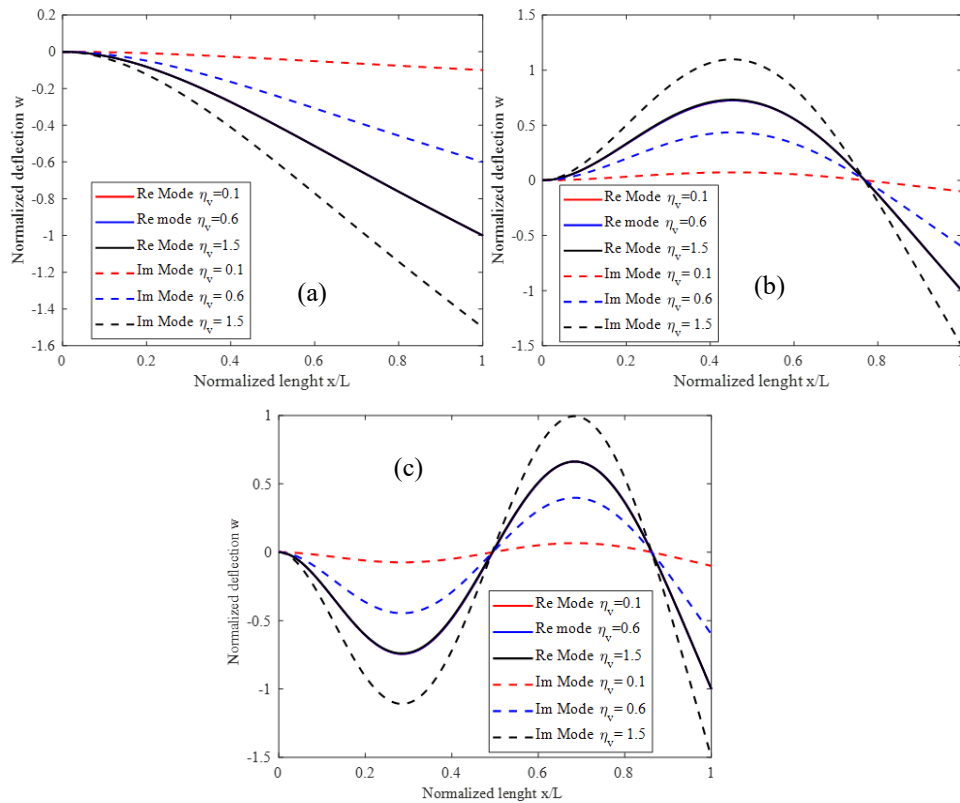


Fig. 3 The complex normalized eigenmodes of C-F VE sandwich beam with $\eta_v = [0.1, 0.6, 1.5]$ (a) mode 1; (b) mode 2; (c) mode 3

4.1.2. Case Study #2: S-S VE Sandwich Beam

For the same mechanical and geometrical properties shown in Table 1, the linear vibration characterizations of S-S supported boundary VE sandwich beam are considered. In this study, based on Rao analytical model [37], the prediction accuracy of the natural frequency and loss factor of the VE sandwich beam structure are compared. It is seen from Tables 5 and 6 that all models, had high accuracy in calculating the first six natural frequencies of VE sandwich beam in comparison with analytical solution [37]. For S-S boundary condition, CPS8 had 0.59% average relative error and C3D20 had the lowest accuracy of 3.6%. On the other hand, from Table 6 it was noticed that both models had relatively high accuracy in predicting the first six loss factors of S-S VE sandwich beam compared with analytical solution [37]. As a result, it means that the prediction accuracy of the numerical approaches for the natural frequency of S-S VE sandwich beam in this work is ranked as follows: CPS8 > C3D20. The dynamic characteristics of VE sandwich beam were studied, and the natural frequency of VE sandwich beam system was larger under S-S boundary conditions. The fundamental loss factor of VE sandwich beams with C-F boundary conditions was higher than that for VE sandwich beams with S-S boundary

conditions. For high values of loss factor of VE material, the imaginary part of the stiffness matrix was considered which implied the existence of not only storage modulus but, also loss modulus. As can be noticed from Fig. 4, the first normalized fundamental complex vibration modes of S-S VE sandwich beam with different damping factor of VE core $\eta_v = [0.1, 0.6, 1.5]$ using the 2D plan stress element CPS8 implemented in Abaqus. The results show that the relative amplitude difference between real and imaginary modes was increased as the loss factor increased so that the imaginary part of the complex fundamental vibration modes was significant and could not be neglected.

The flowchart of the employed methodology for dynamics analysis of sandwich beam is shown in Fig. 5. In the pre-processing stage, material model and tie constraints between the layers are defined. Also, the process involves assigning appropriate element models and defining C-C and S-S boundary conditions. In post-processing, the free vibration response results are interpreted based on tracking model effective mass. In addition, the parametric study stage involves investigation of VE parameters' effects on free vibration response of sandwich beam. In the last stage, steady state forced vibration response with different values of η_v is obtained by utilizing mode superposition method that implies the representation of each eigenmode as an independent pattern of motion.

Table 5 Linear frequencies of S-S VE sandwich beam with different η_v

η_v	Analytical [37]	CPS8 element	C3D20 element
	$\omega_n(Hz)$	$\omega_n(Hz)$	$\omega_n(Hz)$
0.1	148.51	148.44	148.55
	488.47	488.19	489.797
	1034.69	1033.5	1040.57
	1795.13	1791.56	1408.3
	2771.49	2763	2288.4
	3964.28	3946.95	3388.7
0.6	150.71	149.23	149.34
	489.75	489.01	490.61
	1035.38	1034.01	1041.08
	1795.54	1791.89	1811.05
	2771.76	2763.23	2802.92
	3964.47	3947.11	4016.7
1	154.42	150.62	150.73
	492.06	490.48	492.08
	1036.63	1034.95	1042.02
	1796.3	1792.5	1811.65
	2772.27	2763.64	2803.33
	3964.83	3947.41	4016.99
1.5	160.72	153.16	153.27
	496.49	493.29	494.89
	1039.07	1036.78	1043.84
	1797.78	1793.68	1812.82
	2773.25	2764.45	2804.12
	3965.52	3947.99	4017.55
Average Error (%) \approx		0.59	3.60

Table 6 Normalized loss factor of S-S VE sandwich beam with different η_v

η_v	Analytical [37]	CPS8 element	C3D20 element
	η_n/η_v	η_n/η_v	η_n/η_v
0.1	0.107	0.1069	0.1063
	0.065	0.0651	0.0644
	0.043	0.0433	0.0426
	0.031	0.0307	0.03
	0.3328	0.3468	0.3465
	0.1943	0.195	0.1945
0.6	0.1068	0.1068	0.1062
	0.0652	0.0651	0.0644
	0.0433	0.0433	0.0426
	0.0308	0.0307	0.03
	0.305	0.3405	0.3402
	0.192	0.1938	0.1933
1	0.106	0.1066	0.106
	0.065	0.0651	0.0644
	0.043	0.0433	0.0426
	0.031	0.0307	0.03
	0.2626	0.3292	0.27
	0.1871	0.1916	0.231
1.5	0.1059	0.1063	0.15
	0.065	0.065	0.087
	0.0433	0.0432	0.056
	0.0308	0.0307	0.038
	0.0410	0.0432	0.0510
	3346	3333.9	3390
	Average Error (%) \approx	1.8	6.28

4.1.3. Case Study #3: Four-Sided S-S Sandwich Plate

The material and geometrical specifications of SSSS VE plate structure are shown in Table 7. The natural frequencies and loss factors of the structure are calculated using the developed FE model implemented in Abaqus and compared with the results obtained by Johnson and Kienholz [38], who used modal strain energy method (MSE) implemented in NASTRAN commercial software to calculate the natural frequency and loss factor of VE sandwich structures.

The VE sandwich plate in this study is discretized into 2200×120 and 1050×255 meshed areas using C3D20 element along with the length and width directions during the calculation. In addition, the mesh specification of C3D20 element elements implemented in Abaqus is shown in Table 2.

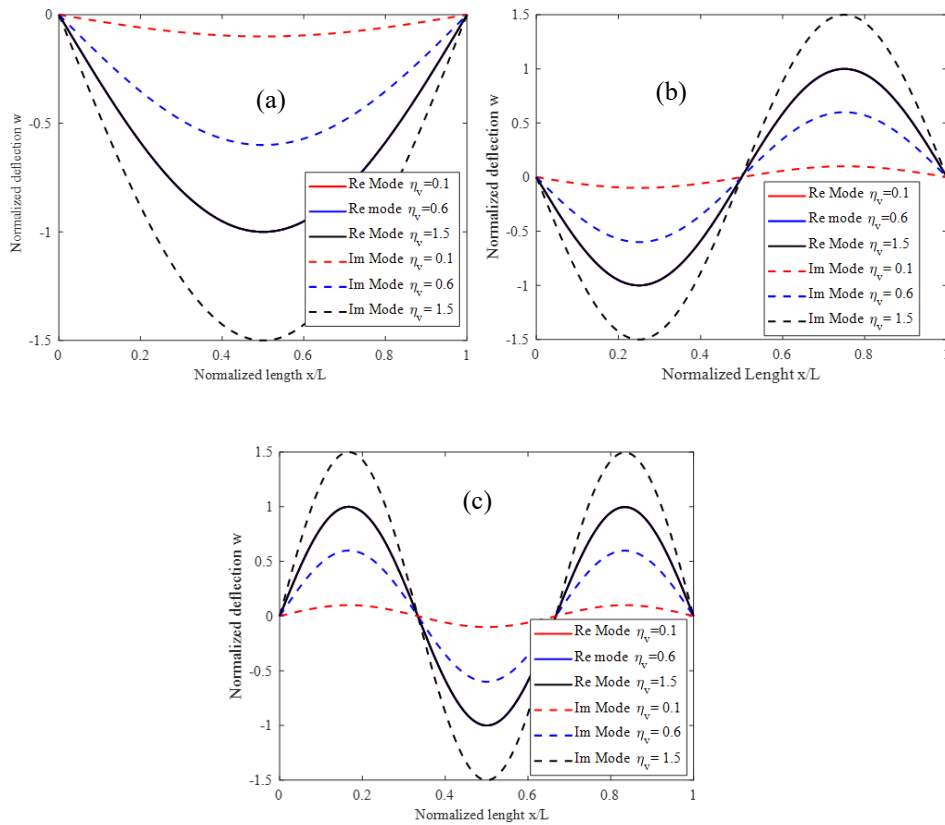


Fig. 4 The complex normalized eigenmodes of S-S VE sandwich beam with $\eta_v = [0.1, 0.6, 1.5]$ (a) mode 1; (b) mode 2; (c) mode 3

Table 7 Mechanical and geometrical specifications of VE SSSS VE sandwich plate [38]

Properties	Elastic layers	VE core layer
Young modulus (Pa)	6.89×10^{10}	1.794×10^6
Poisson's ration	0.3	0.49
Density (kg / m ³)	2740	999
Loss factor	-	0.5
Length (mm)	348	348
Width (mm)	304.8	304.8
Thickness (mm)	0.762	0.254

The mode shapes of the VE sandwich plate associated with the first fundamentals natural frequency obtained using C3D20 element are shown in Fig. 6. The sweet spot could be visualized which showed the maximum deformation location points.

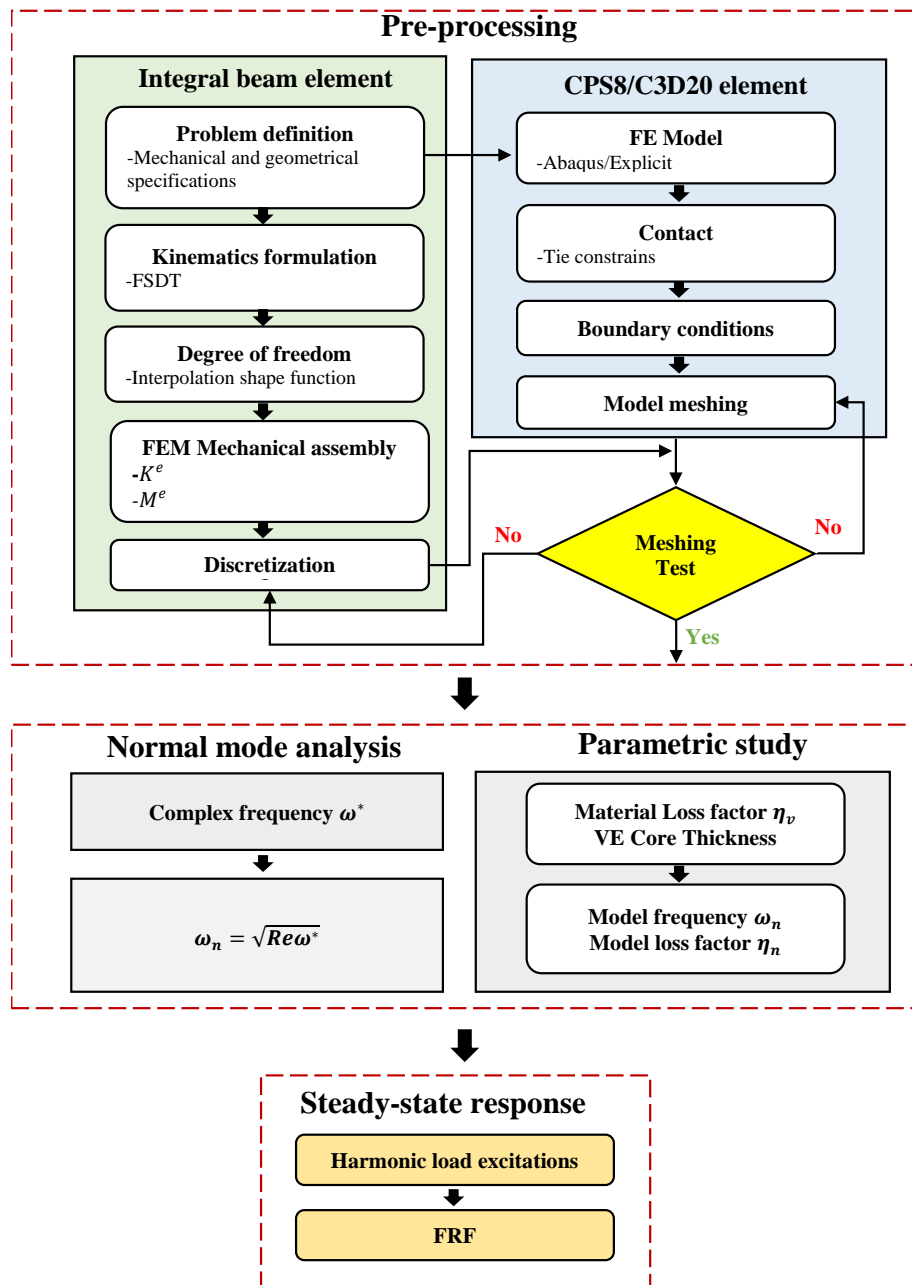


Fig. 5 Flow chart of the proposed dynamics analysis methodology

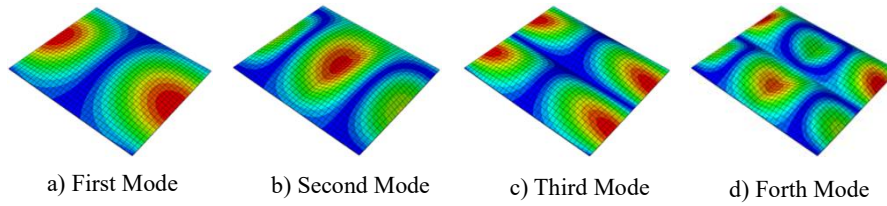


Fig. 6 Fundamental eigenmodes shape of viscoelastic sandwich SSSS plate: (a) First Mode, (b) Second Mode, (c) Third Mode, (d) Forth Mode

Tables 8 and 9 show the calculated results of natural frequency and normalized loss factor, respectively. It is clear from Tables 8 and 9 that C3D20 element had good accuracy in predicting the damping characteristics of VE sandwich SSSS plate against analytical solution with an average error in predicting the fundamental natural frequency of less than 0.4% and an average error of less than 6.5% in predicting the damping loss factor η_n/η_v of VE sandwich plate. In addition, it can be noticed from Tables 8 and 9 that, while increasing the mesh size the error slightly decreases but this increases the time computation of the whole FE process. Thus, there exists a trade-off between mesh refinement and computational efficiency in the FE analysis.

Table 8 Linear complex natural frequencies of VE sandwich plate obtained for different mesh sizes of C3D20 element

Mode	MSE method [38]	C3D20 2200×120		C3D20 1050×255	
	Natural frequency ω_n (Hz)	Natural frequency ω_n (Hz)	Error (%)	Natural frequency ω_n (Hz)	Error (%)
1	57.4	57.3	0.174	57.2	0.348
2	113.2	113.5	0.265	113.3	0.088
3	129.3	129.5	0.155	129.1	0.155
4	179.3	177.7	0.892	177.1	1.227
Average			0.372		0.454

Table 9 Normalized loss factor of VE sandwich plate obtained for different mesh sizes of C3D20 element

Mode	MSE method [38]	C3D20 2200×120		C3D20 1050×255	
	Loss factor η_n/η_v	Loss factor η_n/η_v	Error (%)	Loss factor η_n/η_v	Error (%)
1	0.352	0.366	3.98	0.366	3.963
2	0.376	0.394	4.79	0.396	5.342
3	0.376	0.390	3.72	0.391	4.038
4	0.306	0.346	13.07	0.348	13.835
Average			6.39		6.794

4.2. Parametric Studies

It is required to examine the effects of various parameters on the vibration characteristics of VE sandwich beam. The thickness of the core and VE core loss factor are varied which affects natural frequency and mode shape.

4.2.1 Effect of VE Material Loss Factor on the Dynamic Characteristics of VE Sandwich Beam

To study the influence of VE loss factor on the dynamic characteristics of natural frequency, VE loss factor is varied in the range of 0.1 to 1.5 and the change trends of natural frequency and normalized loss factor corresponding to the fundamental modes of C-F VE sandwich beam are illustrated in Fig. 7. The fundamental natural frequencies of VE sandwich beams only increased minimally when the loss factor was increased from 0.1 to 1.5, indicating that η_v have little effect on the natural frequencies of VE sandwich beams. Constant complex module $E'(1 + j\eta_v)$, showed that the complex elastic modulus E^* of VE material is directly proportional to the loss factor. In addition, the stiffness of VE layer and the stiffness of the entire VE sandwich beam increased. Since the mass of VE sandwich beam did not vary, the fundamental frequency of the beam was increased. However, as shown in Table 1, the elastic modulus of VE layer was four times lower than the elastic modulus of elastic layers, thus the increase in stiffness induced by the loss factor of VE layer could only make VE sandwich C-F beam stiffer. Under the condition of constant mass, the natural frequencies of VE sandwich C-F beam are only increased slightly with a small increase in stiffness. In addition, when the loss factor of VE material η_v is increased, the normalized loss factor η_n/η_v of VE sandwich beam increased linearly, implying that the loss factor of VE material η_v had a significant impact on the loss factor of VE sandwich beam and energy dissipation capacity of VE material is characterized by its loss factor.

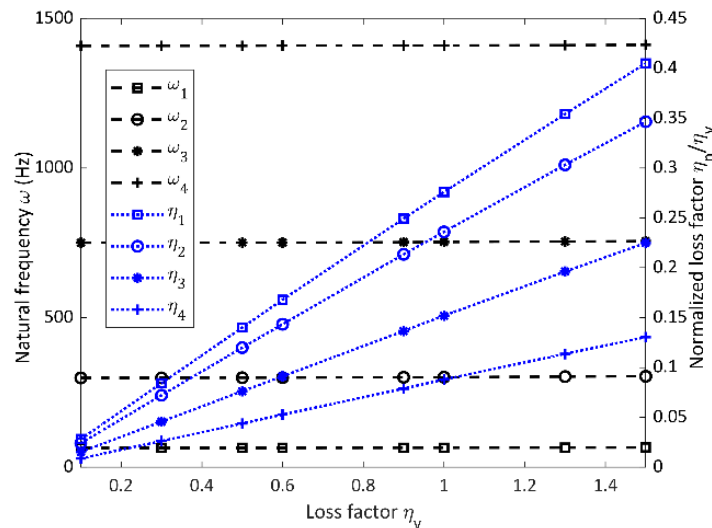


Fig. 7 The effect of η_v on the dynamic characteristics of C-F VE sandwich beam

4.2.2. Effect of VE Core Layer Thickness on the Dynamic Characteristics of VE Sandwich Beam

Core thickness is varied from 0.5 to 6.5 mm to study its influence on the dynamic characteristics ω_n and normalized loss factor η_n/η_v . Indeed, the natural frequency of the system slightly decreased as the thickness of VE layer increased, as seen in Fig. 8. Increase in the stiffness of VE sandwich beam system generated by increasing the thickness of the VE layer was much smaller than the increase in the whole C-F VE sandwich beam stiffness since the elastic modulus of VE layer was four times lower than elastic modulus of elastic layers and the mass of the core was about 50% of elastic layers mass. The changing of the normalized loss factor η_n/η_v for C-F beam was more significant than the changing trend of natural frequency, which was related to the damping nature of VE material.

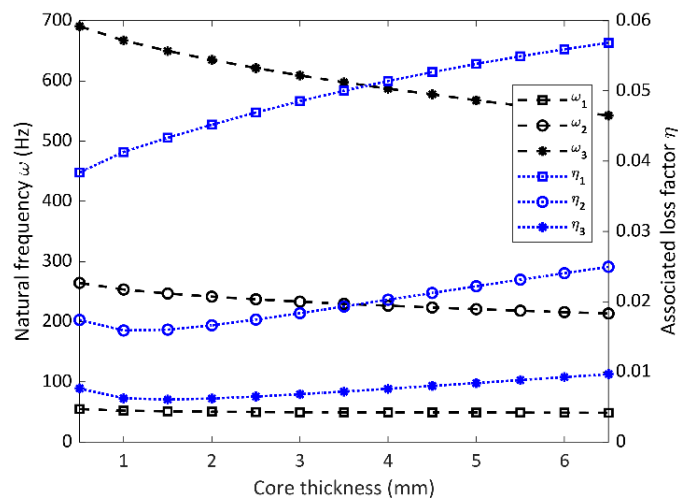


Fig. 8 The effect of core thickness on the dynamic characteristics of C-F VE sandwich beam

4.3. Frequency Response Analysis

Harmonic analysis is required to ensure that the system will successfully overcome resonance and harmful effects and mode superposition method is used based on linear iterations of mode shapes to obtain the frequency response function (FRF). The frequency response curves were then generated to capture the steady-state vibration response of VE sandwich beam across specific frequency range.

4.3.1. Steady-State Dynamics of VE Sandwich Beam/Plate

To excite the first three fundamental mode shapes, a harmonic concentrated force was applied at point $p = (59.27, 6.3)$ mm located along beam length, with magnitude of $F_0 = 100$ N. The system linear frequency response (FRF) is shown in Fig. 9 with different loss factor $\eta_v = [0.3, 0.6, 1]$. It could be noticed from Fig. 9 that the effect of the loss factor was significant, as the system had minimum amplitude response when loss factor $\eta_v = 1$. The maximum response of the system was within the range of the first fundamental natural frequency that had the highest value of effective mass along the direction of applied load.

In addition, Fig. 9 shows that the system tends to vibrate with maximum amplitude at natural frequency values. This occurs since the natural frequency of the structure matches the excitation frequency, leading to a resonance condition that can potentially cause failure effects in the system.

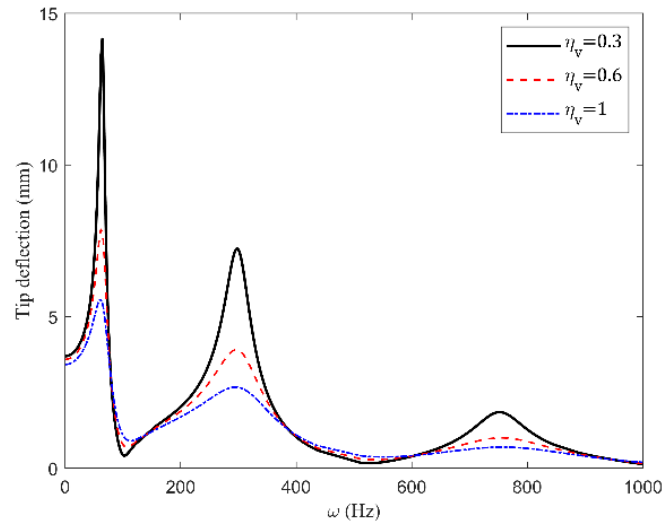


Fig. 9 Linear frequency response curve of fundamental complex modes for C-F VE sandwich beam with $\eta_v = [0.3, 0.6, 0.1]$

5. CONCLUSIONS

In the present work, dynamic analysis was examined to evaluate the damping characteristics of VE sandwich structures, including natural frequency and normalized loss factor η_n/η_v based on longitudinal shear deformation assumption. The obtained numerical results were compared against analytical model to validate the proposed FE models. The numerical results showed that all numerical FE models are applicable for approximating the damping characteristics of VE sandwich beam. The integral shear element model was developed using FE formulation had the lowest error range among other models. In addition, the linear complex natural frequency of VE sandwich plate were obtained for different mesh sizes of C3D20 element. The element shows high accuracy in predicting damping characteristics of VE sandwiched plate structure. Finally, a parametric study was performed to study the effect of various parameters on the dynamic characteristics of VE sandwich beam. The obtained keys conclusion is demonstrated as follows:

- Increasing VE layer thickness decreased the natural frequency and loss factor of the VE sandwich beam.
- The loss factor of VE layer η_v had a significant effect on the overall loss factor of the structure, whereas it had no significant effect on natural frequency.
- The calculated resonance frequencies for VE beam are in the range of modal natural frequency.

In summary, the proposed study provides valuable insights into the dynamics of VE sandwiched structures integrated with aluminum sheets, offering a comprehensive understanding of the factors affecting their damping characteristics.

REFERENCES

1. Cunha-Filho, A.G., De Lima, A.M.G., Donadon, M.V., Leão, L.S., 2016, *Flutter suppression of plates subjected to supersonic flow using passive constrained viscoelastic layers and Golla-Hughes-McTavish method*, Aerospace Science and Technology, 52, pp. 70–80.
2. Kim, S.Y., Kim, S.H., Oh, H.J., Leeh, S.H., Youn, J.R., 2010, *Residual stress and viscoelastic deformation of film insert molded automotive parts*, Journal of Applied Polymer Science, 118(5), pp. 2530–2540.
3. Ye, K., Li, L., Tang, J., 2003, *Stochastic seismic response of structures with added viscoelastic dampers modeled by fractional derivative*, Earthquake Engineering and Engineering Vibration, 2(1), pp. 133–139.
4. Milić, P., Marinković, D., Klinge, S., Čojbašić, Ž., 2023, *Reissner-Mindlin Based Isogeometric Finite Element Formulation for Piezoelectric Active Laminated Shells*, Tehnički vjesnik, 30(2), pp. 416–425.
5. Gröhlich, M., Böswald, M., Wallaschek, J., 2023, *Viscoelastic damping design – A novel approach for shape optimization of constrained layer damping treatments at different ambient temperatures*, Journal of Sound and Vibration, 555, 117703.
6. Ganguly, K., Roy, H., 2021, *Modelling and analysis of viscoelastic laminated composite shaft: an operator-based finite element approach*, Archive of Applied Mechanics, 91(1), pp. 343–362.
7. Wang, F., Liao, J., Huang, C., Yu, H., Yan, J., Li, H., 2022, *Study on the damping dynamics characteristics of a viscoelastic damping material*, Process, 10(4), 635.
8. Zenkour, A.M., El-Mekawy, H.F., 2018, *Stresses in inhomogeneous elastic–viscoelastic–elastic sandwich plates via hyperbolic shear deformation theory*, Journal of the Brazilian Society of Mechanical Sciences and Engineering, 40(7), 363.
9. Marinkovic, D., Zehn, M., Marinkovic, Z., 2012, *Finite element formulations for effective computations of geometrically nonlinear deformations*, Advances in Engineering Software, 50(1), pp. 3–11.
10. Safaei, B., Onyibo, E.C., Hurdoganoglu, D., 2022, *Effect of static and harmonic loading on the honeycomb sandwich beam by using finite element method*, Facta Universitatis-Series Mechanical Engineering, 20(2), pp. 279–306.
11. Safaei, B., Onyibo, E.C., Hurdoganoglu, D., 2022, *Thermal buckling and bending analyses of carbon foam beams sandwiched by composite faces under axial compression*, Facta Universitatis-Series Mechanical Engineering, 20(3), pp. 589–615.
12. Safaei, B., Onyibo, E.C., Goren, M., Kotrasova, K., Yang, Z., Arman, S., Asmael, M., 2023, *Free vibration investigation on RVE of proposed honeycomb sandwich beam and material selection optimization*, Facta Universitatis-Series Mechanical Engineering, 21(1), pp. 31–50.
13. Arvin, H., Sadighi, M., Ohadi, A.R., 2010, *A numerical study of free and forced vibration of composite sandwich beam with viscoelastic core*, Composite Structures, 92(4), pp. 996–1008.
14. Wang, Y., Inman, D.J., 2013, *Finite element analysis and experimental study on dynamic properties of a composite beam with viscoelastic damping*, Journal of Sound and Vibration, 332(23), pp. 6177–6191.
15. Lin, F., Rao, M.D., 2010, *Vibration analysis of a multiple-layered viscoelastic structure using the biot damping model*, AIAA Journal, 48(3), pp. 624–634.
16. Shashidhar, R.R., Panda S., 2023, *A generalized finite element formulation for nonlinear frequency response analysis of viscoelastic sandwich beams using harmonic balance method*, Archive of Applied Mechanics, 93, pp. 2209–2241.
17. Jahan, A., Kuchak, T., Dragan, M., Zehn, M., 2021, *Parametric investigation of a rail damper design based on a lab-scaled model*, Journal of Vibration Engineering & Technologies, 9(1), pp. 51–60.
18. Araújo, A.L., Mota Soares, C.M., Mota Soares, C.A., 2010, *A viscoelastic sandwich finite element model for the analysis of passive, active and hybrid structures*, Applied Composite Materials, 17(5), pp. 529–542.
19. Lewandowski R, Baum M, 2015, *Dynamic characteristics of multilayered beams with viscoelastic layers described by the fractional Zener model*, Archive of Applied Mechanics, 85(12), pp. 1793–1814.
20. Daya E.M, Potier-Ferry M, 2002, *A shell finite element for viscoelastically damped sandwich structures*, Revue Européenne des Elements, 11(1), pp. 39–56.
21. Koutsawa, Y., Charpentier, I., Daya, E.M., Cherkaoui, M., 2008, *A generic approach for the solution of nonlinear residual equations part I: the Diamant toolbox*, Computer Methods in Applied Mechanics and Engineering, 198(3), pp. 572–577.

22. Lampoh, K., Charpentier, I., Daya, E.M., 2011, *A generic approach for the solution of nonlinear residual equations. part III: sensitivity computations*, Computer Methods in Applied Mechanics and Engineering 200(45-46), pp. 2983–2990.
23. Loghman, E., Bakhtiari-Nejad, F., Kamali, E.A., Abbaszadeh, M., Amabili, M., 2021, *Nonlinear vibration of fractional viscoelastic micro-beams*, International Journal of Non-Linear Mechanics, 137, 103811.
24. Li, H., Li, Z., Safaei, B., Rong, W., Wang, W., Qin, Z., Xiong, Z., 2021, *Nonlinear vibration analysis of fiber metal laminated plates with multiple viscoelastic layers*, Thin-Walled Structures, 168, 108297.
25. Rahmani, A., Safaei, B., Qin, Z., 2022, *On wave propagation of rotating viscoelastic nanobeams with temperature effects by using modified couple stress-based nonlocal Eringen's theory*, Engineering with Computers, 38(4), pp. 2681–2701.
26. Yuan, Y., Zhao, X., Zhao, Y., Sahmani, S., Safaei, B., 2021, *Dynamic stability of nonlocal strain gradient FGM truncated conical microshells integrated with magnetostrictive facesheets resting on a nonlinear viscoelastic foundation*, Thin-Walled Structures, 159, 107249.
27. Jalaei, M.H., Thai, H.T., Civalek, 2022, *On viscoelastic transient response of magnetically imperfect functionally graded nanobeams*, International Journal of Engineering Science, 172, 103629.
28. Youzera, H., Selim Saleh, M.M., Ghazwani, M.H., Meftah, S.A., Tounsi, A., Cuong-Le, T., 2023, *Nonlinear damping and forced vibration analysis of sandwich functionally graded material beams with composite viscoelastic core layer*, Mechanics Based Design of Structures and Machines, doi:10.1080/15397734.2023.2229911.
29. Karmi, Y., Tekili, S., Khadri, Y., Boumediri, H., 2023, *Vibroacoustic analysis in the thermal environment of PCLD sandwich beams with frequency and temperature dependent viscoelastic cores*, Journal of Vibration Engineering & Technologies, doi:10.1007/s42417-023-01065-6.
30. Chen, Q., Chan Y.W., 2000, *Integral finite element method for dynamical analysis of elastic–viscoelastic composite structures*, Computers & Structures, 74(1), pp. 51–64.
31. Baber, T.T., Maddox, R.A., Orozco, C.E., 1998, *A finite element model for harmonically excited viscoelastic sandwich beams*, Computers & Structures; 66(1), pp. 105–113.
32. Huang, Z., Qin, Z., Chu, F., 2016, *Damping mechanism of elastic-viscoelastic-elastic sandwich structures*, Composite Structures, 153, pp. 96–107.
33. Daya, E.M., Potier-Ferry M., 2001, *Numerical method for nonlinear eigenvalue problems application to vibrations of viscoelastic structures*, Computers and Structures, 79(5), pp. 533–541.
34. Soni, M.L., Bogner, F.K., 1982, *Finite element vibration analysis of damped structures*, AIAA Journal 20(5), pp. 700–707.
35. Abdoun, F., Azrar, L., Daya, E.M., Potier-Ferry, M., 2008, *Forced harmonic response of viscoelastic structures by an asymptotic numerical method*, Computers & Structures, 87(1-2), pp. 91-100.
36. Bilasse, M., Daya, E.M., Azrar, L., 2010, *Linear and nonlinear vibrations analysis of viscoelastic sandwich beams*, Journal of Sound and Vibration, 29(23), pp. 4950-4969.
37. Rao, D.K., 1978, *Frequency and loss factors of sandwich beams under various boundary conditions*, Journal of Mechanical Engineering Science, 20(2), pp. 271–282.
38. Johnson, C., Kienholz, D., 1982, *Finite element prediction of damping in structures with constrained viscoelastic layers*, AIAA Journal, 20(9), pp. 1284–1290.